

Article

Not peer-reviewed version

# Integrated Smart Gas Tracking Device with Artificially Tailored Selectivity for Real-Time Monitoring Food Freshness

[Yuli Xu](#) , Zicheng Liu , Jingren Lin , Jintao Zhao , Nguyen Duc Hoa , Nguyen Van Hieu , Alexander A. Ganeev , [Victoria Chuchina](#) , [Abolghasem Jouyban](#) , [Daxiang Cui](#) , [Ying Wang](#) \* , [Han Jin](#) \*

Posted Date: 20 September 2023

doi: 10.20944/preprints202308.1734.v2

Keywords: artificially tailored selectivity; smart gas sensor; yttria-stabilized zirconia (YSZ); volatile compounds; food freshness



Preprints.org is a free multidiscipline platform providing preprint service that is dedicated to making early versions of research outputs permanently available and citable. Preprints posted at Preprints.org appear in Web of Science, Crossref, Google Scholar, Scilit, Europe PMC.

Copyright: This is an open access article distributed under the Creative Commons Attribution License which permits unrestricted use, distribution, and reproduction in any medium, provided the original work is properly cited.

Disclaimer/Publisher's Note: The statements, opinions, and data contained in all publications are solely those of the individual author(s) and contributor(s) and not of MDPI and/or the editor(s). MDPI and/or the editor(s) disclaim responsibility for any injury to people or property resulting from any ideas, methods, instructions, or products referred to in the content.

## Article

# Integrated Smart Gas Tracking Device with Artificially Tailored Selectivity for Real-Time Monitoring Food Freshness

Yuli Xu <sup>1</sup>, Zicheng Liu <sup>1,†</sup>, Jingren Lin <sup>1,†</sup>, Jintao Zhao <sup>1</sup>, Nguyen Duc Hoa <sup>2</sup>, Nguyen Van Hieu <sup>3</sup>, Alexander A. Ganeev <sup>4</sup>, Victoria Chuchina <sup>4</sup>, Abolghasem Jouyban <sup>5</sup>, Daxiang Cui <sup>1,6</sup>, Ying Wang <sup>7,8,\*</sup> and Han Jin <sup>1,6,\*</sup>

<sup>1</sup> Institute of Micro-Nano Science and Technology, School of Electronic Information and Electrical Engineering, Shanghai Jiao Tong University, Shanghai 200240, China

<sup>2</sup> International Training Institute for Material Science, Hanoi University of Science and Technology, Hanoi, Vietnam

<sup>3</sup> Faculty of Electrical and Electronic Engineering, Phenikaa University, Hanoi, Vietnam

<sup>4</sup> St Petersburg University, 7/9 Universitetskaya Emb., St Petersburg 199034, Russia

<sup>5</sup> Pharmaceutical Analysis Research Center and Faculty of Pharmacy, Tabriz University of Medical Sciences, Tabriz, Iran

<sup>6</sup> National Engineering Research Center for Nanotechnology, Shanghai, 200241, P. R. China

<sup>7</sup> Chengdu Environmental Investment Group Co., LTD, Building 1, Tianfushijia, No. 1000 Jincheng Street, Chengdu, China

<sup>8</sup> Department of Biological Science, College of Life Sciences, Sichuan Normal University, Chengdu 610101, Sichuan, China

\* Correspondence: wangyingcqu@gmail.com (Y.W.); jinhan10@sjtu.edu.cn (H.J.)

† These authors contributed equally.

**Abstract:** The real-time monitoring of food freshness in refrigerators is of significant importance in detecting potential food spoiling and preventing serious health issues. One method that is commonly reported and has received substantial attention is the discrimination of food freshness by the tracking of volatile molecules. Nevertheless, the ambient environment of low temperature (normally below 4°C) and high humidity (90% R.H.) as well as poor selectivity in sensing gas species remain the challenge. In this research, an integrated smart gas-tracking device is designed and fabricated. By applying pump voltage on the yttria-stabilized zirconia (YSZ) membrane, the oxygen concentration in the testing chamber can be manually tailored. Due to the working principle of the sensor following the mixed potential behavior, distinct differences in sensitivity and selectivity are observed for the sensor that operated at different oxygen concentrations. Typically, the sensor gives satisfactory selectivity to H<sub>2</sub>S, NH<sub>3</sub>, and C<sub>2</sub>H<sub>5</sub>OH at the oxygen concentrations of 10%, 30%, and 40%, respectively. In addition, an acceptable response/recovery rate (within 24 s) is also confirmed. Finally, a refrigerator prototype that includes the smart gas sensor is built, and satisfactory performance in discriminating food freshness status of fresh or semi-fresh is verified for the proposed refrigerator prototype. In conclusion, these aforementioned promising results suggest that the proposed integrated smart gas sensor could be a potential candidate for alarming food spoilage.

**Keywords:** artificially tailored selectivity; smart gas sensor; yttria-stabilized zirconia (YSZ); volatile compounds; food freshness

## 1. Introduction

The issue of food freshness has garnered significant attention due to its direct impact on human health and safety. [1] In the context of urban living, it is common practice to store various food items in a refrigerator and subsequently consume them over a specific duration. Nevertheless, it is important to note that different types of food have the potential to deteriorate over a period of time. This degradation may go unnoticed by individuals due to the relatively airtight conditions within a refrigerator, hindering their ability to detect any visual or olfactory signs of rotting. The occurrence



of food spoilage in refrigerated storage facilities contributes significantly to the annual volume of food waste, while the consumption of such deteriorated food items can lead to the manifestation of severe health complications. Therefore, Real-time monitoring of the freshness of food stored in the refrigerator is of great significance since it will be helpful to alarming the potential food spoilage, and thereby can effectively prevent severe health problems (e.g. food poisoning) that may be caused by eaten rotten food.[2,3]

There are several elements that might influence the freshness of food, including microorganisms, temperature, humidity, and storage conditions. Hence, the assessment of food freshness within the refrigerator is a highly intricate process.[4] The microbiological and chemical processes like changes in protein and lipid fractions, are mainly responsible for the spoilage of fresh food.[5] Up to date, methods that have been frequently reported for food freshness monitoring include but are not limited to microbiological testing, visual recognition, capillary electrochromatography, volatile compounds analysis, *etc.*[6–11] Among them, discriminating food freshness through tracking volatile compounds receives extensive attention due to its attractive characteristics of rapid and non-invasive which are suitable for alarming food spoilage at an early stage. [12–14] Traditionally, the analysis of volatile substances has been conducted using several methods such as gas chromatography (GC), [15] ion mobility spectrometry (IMS),[8] and proton-transfer-reaction mass spectrometry (PTR-MS).[16] These methodologies offer a both qualitative and quantitative assessment of volatile substances, however, they necessitate the involvement of skilled individuals and entail significant operational expenses[17]. Additionally, the sample preparation and analysis procedures associated with these approaches are time-consuming. In addition, it should be noted that these devices possess a substantial size and necessitate regular calibration.[18–20] This has motivated significant efforts for the development of gas sensors that may offer a more rapid, user-friendly, miniaturized, non-destructive, and affordable detection of several important gases with high selectivity and sensitivity.[21] To present, high-performance silicon transistor arrays for trace-level, multi-gas sensing have effectively assessed food freshness in complex gaseous environments for practical applications.[22] However, in consideration of the ambient environment of low temperature (normally below 4°C) and high humidity (90% R.H.) in refrigerators, it is highly desired to develop high-performance chemical gas sensors when tracking target volatile gas species.[7,9,14,23–25]

When food is refrigerated, some components disintegrate and emit odors as a result of the reaction of bacteria and enzymes. Proteins undergo degradation, resulting in the formation of spoilage amines, which then break down into ammonia, hydrogen sulfide, and ethyl mercaptan.[26] The process of fat decomposition involves the breakdown of fat molecules into fatty acids, which are subsequently converted into aldehydes.[27] Carbohydrates undergo decomposition processes that result in the formation of alcohols, ketones, and aldehydes.[28] Therefore, to effectively monitor food freshness, three main target volatile compounds should be particularly focused on, namely, H<sub>2</sub>S (derived from meat spoilage), NH<sub>3</sub> (derived from meat spoilage), and C<sub>2</sub>H<sub>5</sub>OH (derived from vegetable/fruit spoilage).[1,29] In comparison with chemiresistive-type gas sensors, solid-state yttria-stabilized zirconia (YSZ) based gas sensors demonstrate reliable performance in harsh conditions.[4,30–35] In addition, because of the relatively high selectivity, it is expected that YSZ-based gas sensors could be a promising candidate for sensing these volatile compounds in refrigerators.[36–39] Nevertheless, highly selective tracking of the aforementioned H<sub>2</sub>S, NH<sub>3</sub>, and C<sub>2</sub>H<sub>5</sub>OH against other potential co-existing interference gases, like CO, NO, NO<sub>2</sub>, and SO<sub>2</sub> remains a challenge.[40–42]

It is widely recognized that gas sensors based on yttria-stabilized zirconia (YSZ) typically exhibit mixed potential behavior when exposed to gas mixtures containing oxygen.[40,43–45] Consequently, the sensing characteristics (i.e., sensitivity and selectivity) of this type of sensor could be manipulated artificially by varying the oxygen concentration in the gas mixture.[43,46] In consequence, this research proposes an integrated smart gas sensor with artificially tailored selectivity for monitoring volatile compounds typically generated during food deterioration. Using a YSZ membrane to control the oxygen concentration in the testing chamber, an integrated ceramic-based oxygen pump is created so that the selectivity of a miniaturized YSZ-based electrochemical gas sensor can be readily

adjusted. In the interim, the practicability of the integrated smart gas sensor to monitor the level of food preservation in the refrigerator will be systematically assessed. This research is believed to provide an alternative strategy for designing high-performance gas sensors for future food quality evaluation applications.

## 2. Experimental Section

### 2.1. Materials preparation

Materials (e.g.  $\text{SnO}_2$ ,  $\text{Co}_3\text{O}_4$ ,  $\text{ZnO}$ ,  $\text{NiO}$ ,  $\text{Cr}_2\text{O}_3$ , and  $\text{In}_2\text{O}_3$ ) whose sensing behavior is widely reported to be easily affected by oxygen concentration were selected as research objectives. All the materials are directly bought from Sigma-Aldrich.

### 2.2. Fabrication of the Integrated Smart Gas Sensor

The intelligent gas sensor is composed of two parts, namely, a testing chamber (chamber oxygen concentration controlling module) and a miniaturized YSZ-based sensor (target gas sensing module). The fabrication details of each part are summarized as follows:

(i) *Fabrication of the chamber oxygen concentration controlling module*: Initially, Pt paste (Tanaka, Japan) and  $\text{Mn}_2\text{O}_3$  paste were painted on the surface of commercial YSZ plates (length  $\times$  width  $\times$  thickness:  $1.75 \times 0.5 \times 0.1 \text{ cm}^3$ ; Nikkato, Japan) to form the oxygen pumping and sensing electrode. After that, two pieces of the as-fabricated commercial YSZ plates were bound together with the help of glass cement, followed by calcined at  $1400^\circ\text{C}$  for 2.5 h to form the chamber oxygen concentration controlling module. The space of the internal testing chamber is about  $0.06 \text{ cm}^3$  (length  $\times$  width  $\times$  thickness:  $1.5 \times 0.4 \times 0.1 \text{ cm}^3$ ; as shown in Figure 1).

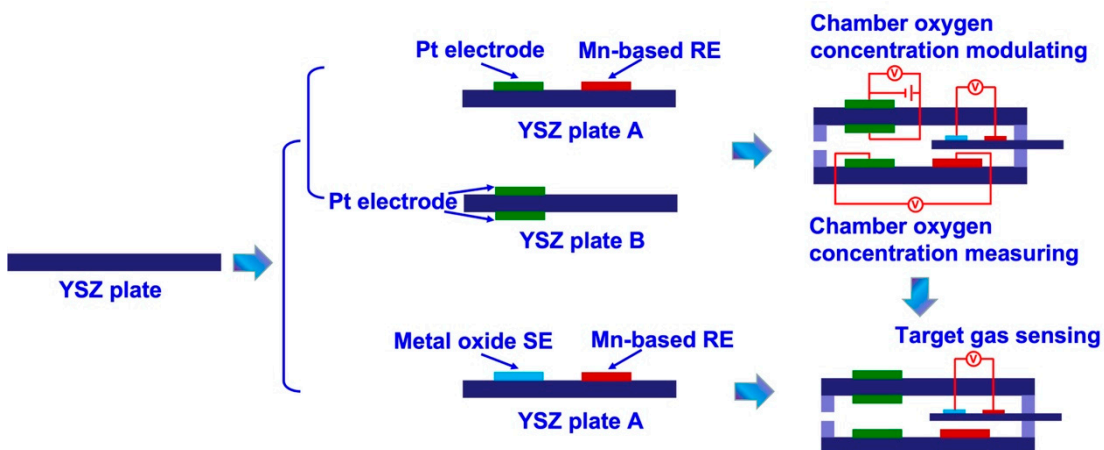


**Figure 1.** Schematical view of the details of fabricating the integrated smart gas sensors.

(ii) *Fabrication of the target gas sensing module and integrated smart gas sensor*: YSZ-based sensors are fabricated by using commercial YSZ plates (length  $\times$  width  $\times$  thickness:  $2 \times 0.3 \times 0.1 \text{ cm}^3$ ; Nikkato, Japan). To simplify the configuration of the fabricated sensors, manganese-based reference-electrode (hereafter denoted as Mn-based RE) was used on these sensors. A commercially available  $\text{Mn}_3\text{O}_4$  powder (99% purity, Sigma, Germany) was meticulously blended with  $\alpha$ -terpineol. The resulting paste was subsequently applied onto the surface of YSZ plates, resulting in the formation of a  $1 \text{ mm}$   $\text{Mn}_3\text{O}_4$ -banded electrode. After undergoing a drying process at a temperature of  $130^\circ\text{C}$  for an entire night, YSZ plates that contained a layer of  $\text{Mn}_3\text{O}_4$  were subjected to calcination at a temperature of  $1400^\circ\text{C}$  for 2.5 hours in an environment consisting of air. This calcination process aimed to facilitate the formation of the Mn-based RE. Each of the sensing materials, namely  $\text{SnO}_2$ ,  $\text{Co}_3\text{O}_4$ ,  $\text{ZnO}$ ,  $\text{NiO}$ ,  $\text{Cr}_2\text{O}_3$ , and  $\text{In}_2\text{O}_3$  (purchased from Sigma, Germany, with a purity of 99%), which were based on metal oxides, were individually applied onto the surface of the YSZ plates. This application was done to create an oxide layer that possessed similar dimensions to the Mn-based RE. Subsequently, each of

the fabricated oxide layers underwent calcination at high temperatures to obtain the photoactive SEs. The calcination temperature for the  $\text{Cr}_2\text{O}_3$ -SE sensor ranged from 900 to 1100°C, while for the sensor composed of the other SEs, the calcination temperature was fixed at 1000°C. Subsequently, the YSZ-based sensors, in their as-fabricated state, were carefully placed within the testing chamber and securely sealed using glass cement, resulting in the creation of integrated smart gas sensors. Figure 1 displays a schematic representation of the sensor.

### 2.3. Evaluating the gas sensing performance of the integrated smart gas sensor

Sensing experiments were performed by simultaneously exposing the sensors to the base gas (diluted 21 vol%  $\text{O}_2$  +  $\text{N}_2$  balance) or the sample gas containing each of different volatile compounds in the range of 0.04–2 ppm for each in the based gas to evaluate gas-sensing characteristics. Since  $\text{H}_2\text{S}$ ,  $\text{NH}_3$ , and  $\text{C}_2\text{H}_5\text{OH}$  are the most prevalent volatile compounds emitted during food decomposition, these gas species were chosen as the sample gas for this investigation. The humidity and the temperature of the gas mixture are kept at 90% RH and 4 °C to simulate the operating condition in the refrigerator. To eliminate the negative impact derived from humidity and low ambient temperature, the sensor is operated at 425 °C through an internal aluminum oxide heating plate.

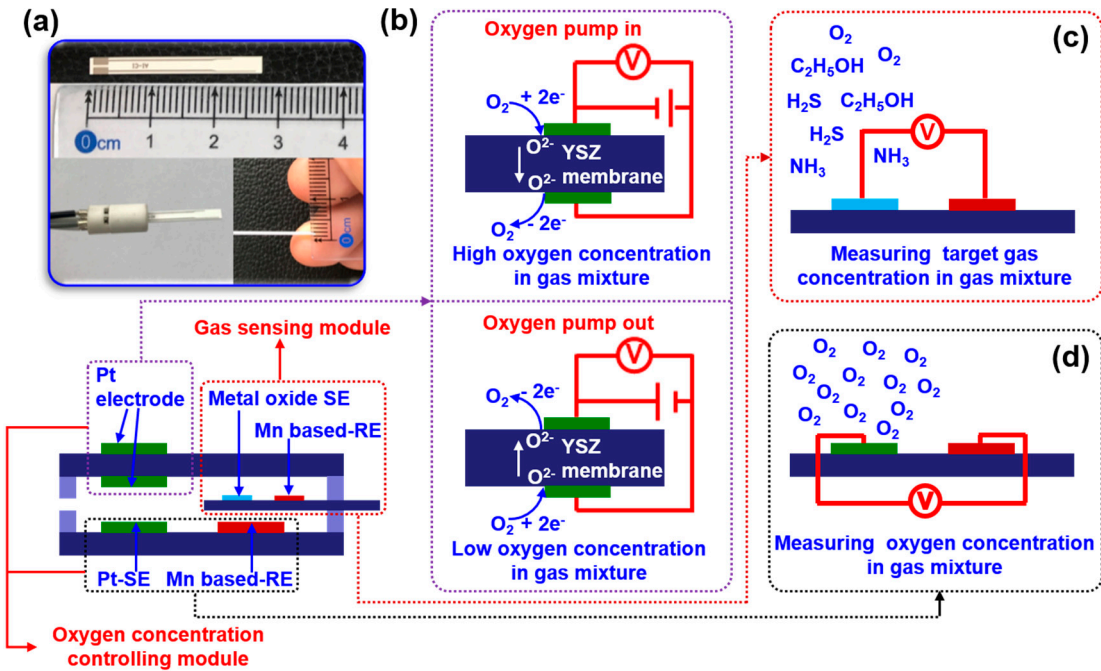
The oxygen concentration inside the testing chamber is manually modulated by applying pumping voltage on the pumping electrode which is located on the surface of the YSZ membrane (Figure 2b). By controlling the pumping time, oxygen concentration in the testing chamber can be artificially fixed in the range of 10–40 %. The sensing signal of electric potential difference  $\Delta V$  ( $\Delta V = V_{\text{sample gas}} - V_{\text{base gas}}$ , where the  $V_{\text{sample gas}}$  represents the sensing response of the sensor towards sample gas, whereas the  $V_{\text{base gas}}$  represents the sensing response of the sensor towards base gas) was recorded by using a multi-function data acquisition board (USB-6211, NI, USA). The 90% response/recovery time was calculated in the following way: the maximum value of the sensor given at response/recovery within the examined time was denoted as the  $\Delta V_{\text{response/recovery}}$ , and then the value of 90%  $\Delta V_{\text{response/recovery}}$  can be read from the figure and its corresponding time was defined as the 90% response/recovery time.

The current–voltage (polarization) curves were measured with an electrochemical analyzer system (CHI604D, Chenhua, China), by employing the linear potential-sweep method at a scan rate of 0.1 mV/s at 475 °C in air base (or sample gas). In brevity, the standard modified polarization curve for the cathodic reaction of air was obtained by plotting the applied potential against the absolute current value. The modified polarization curve for the anodic reaction of the sample gas was estimated by subtracting the current value in the base gas from the current value in the sample gas at each potential.

## 3. Results and discussion

### 3.1. General Vision of the Integrated Smart Gas Sensor

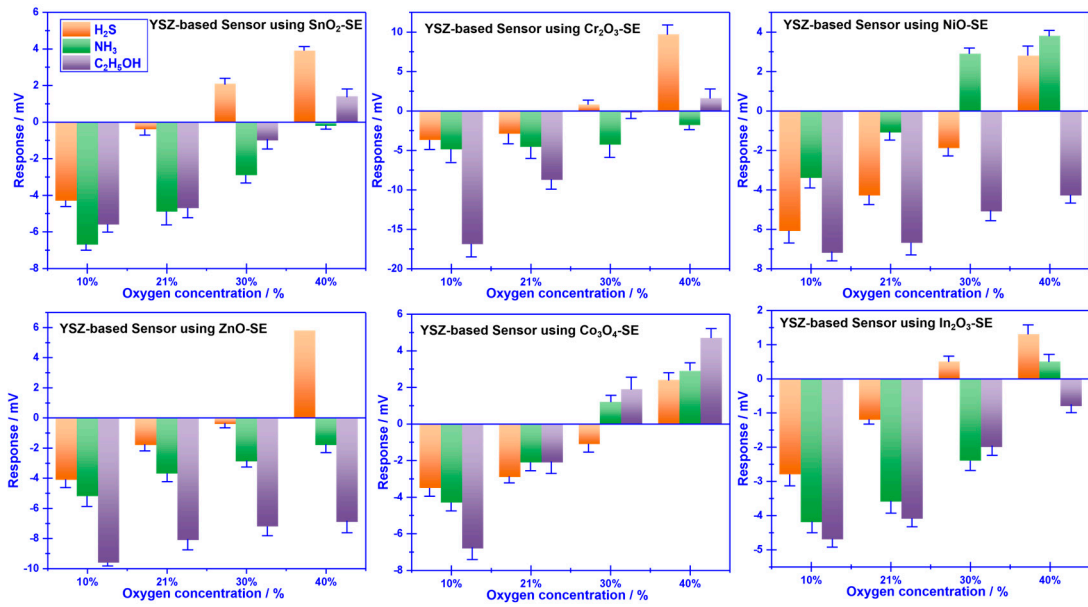
An integrated smart sensor is proposed and designed for food quality monitoring. The proposed sensor is composed of a chamber oxygen concentration controlling module and a target gas sensing module (Figure 2a). When exposing the sensor to the gas mixture, the oxygen concentration in the gas mixture will be automatically modulated with the help of the oxygen concentration controlling module. By applying pumping voltage on the YSZ membrane, oxygen can be controllable and pumped out of or inside the testing chamber, leading to low or high oxygen concentration in the gas mixture (in the testing chamber), as shown in Figure 2b. A gas sensor based on yttria-stabilized zirconia (YSZ) will be developed in a downsized form and integrated into the testing chamber. This sensor aims to achieve superior performance in detecting certain gases, as seen in Figure 2c. Meanwhile, the oxygen concentration within the testing chamber is continuously monitored in real-time to manually adjust it to the desired value. Due to the YSZ-based sensor following the working principle of mixed potential behavior, its sensing characteristics will directly be tailored by the oxygen concentration in the gas mixture (in the testing chamber). Consequently, high selectivity to specific gas at certain oxygen concentration is expected.



**Figure 2.** Illustration of the integrated smart gas sensor. (a) a miniaturized YSZ-based sensor; (b) oxygen pump principle; (c) manually controlling the oxygen concentration in the testing chamber; (d) measuring target gas concentration.

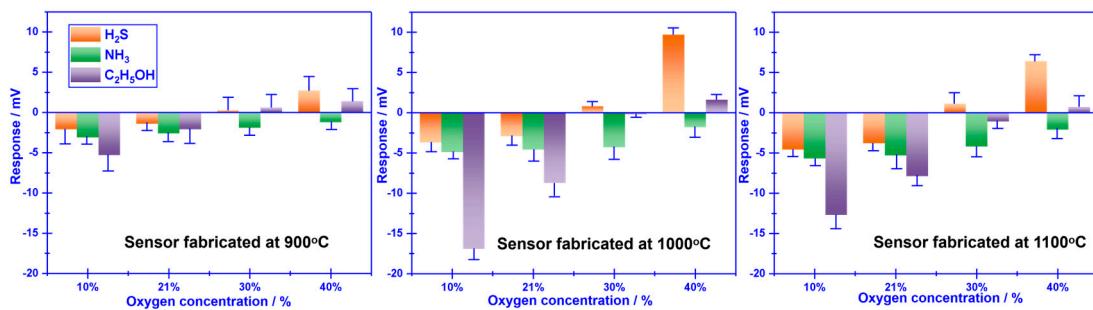
### 3.2. Sensing performance of the proposed smart gas sensor

To realize the aforementioned attractive vision, the sensing behavior of YSZ-based gas sensors using a variety of commonly reported sensing materials (e.g.  $SnO_2$ ,  $Co_3O_4$ ,  $ZnO$ ,  $NiO$ ,  $Cr_2O_3$ , and  $In_2O_3$ ) as the SE (vs Mn-based RE) to 0.04 ppm  $H_2S$ ,  $NH_3$ ,  $C_2H_5OH$  was initially characterized under different oxygen concentrations (10%, 21%, 30% and 40%). As depicted in Figure 3, the response signal of the YSZ-based gas sensors attached with various sensing materials (as the sensing electrode, SE) vs. the Mn-based reference electrode (RE) varied with the oxygen concentration, and most of these sensors exhibited unexpected selectivity towards the studied gases. Nevertheless, it is intriguing to note that the sensor using  $Cr_2O_3$ -SE (vs. Mn-based RE) demonstrated relatively high selectivity to  $H_2S$ ,  $NH_3$ , and  $C_2H_5OH$  at various oxygen concentrations. For instance, the response signal of the sensor to 0.04 ppm  $H_2S$ ,  $NH_3$ ,  $C_2H_5OH$  under the oxygen concentration of 10%, 30%, and 40% is (-3.7 mV, -4.9 mV, -17.3 mV), (0.8 mV, -4.3 mV, -0.2 mV) and (8.7 mV, -1 mV, 1.6 mV), respectively. This encouraging result suggests that it is quite possible to achieve the desired high selectivity for detecting volatile compounds derived from spoiled food by modifying the oxygen concentration in the testing atmosphere.



**Figure 3.** Sensing characteristics of the smart gas sensor attached with various SEs and Mn-based RE, under different oxygen concentrations.

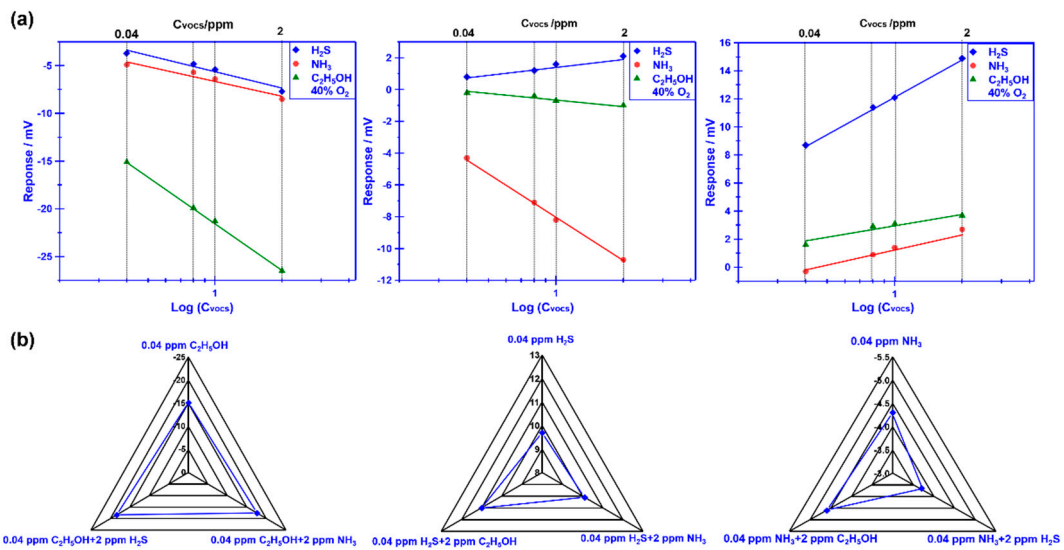
The calcination temperature of the sensor attached with  $\text{Cr}_2\text{O}_3$ -SE is further optimized in the range of 900–1100 °C, with intervals of 100 °C (shown in Figure 4). The largest response signal and optimal selectivity are obtained for the sensor calcined at 1000°C. The impact of calcination temperature can be explained through the balance of forming triple-phase boundary (TPB) and catalytic activity which has been systematically discussed elsewhere.[47] TPB can be hardly formed at low calcination, leading to feeble electrocatalytic activity and low reactivity at the reaction interface (i.e. interface between SE and YSZ). Even so, an excessively high calcination temperature normally destroys the catalytic activity of the sensing materials. As a result, a moderate calcination temperature not only aids in enhancing the interfacial reactivity by forming a desirable TPB but also maintains an adequate level of catalytic activity. Thus, optimal sensing performance is observed at the calcination temperature of 1000 °C for the YSZ-based sensor that is associated with  $\text{Cr}_2\text{O}_3$ -SE.



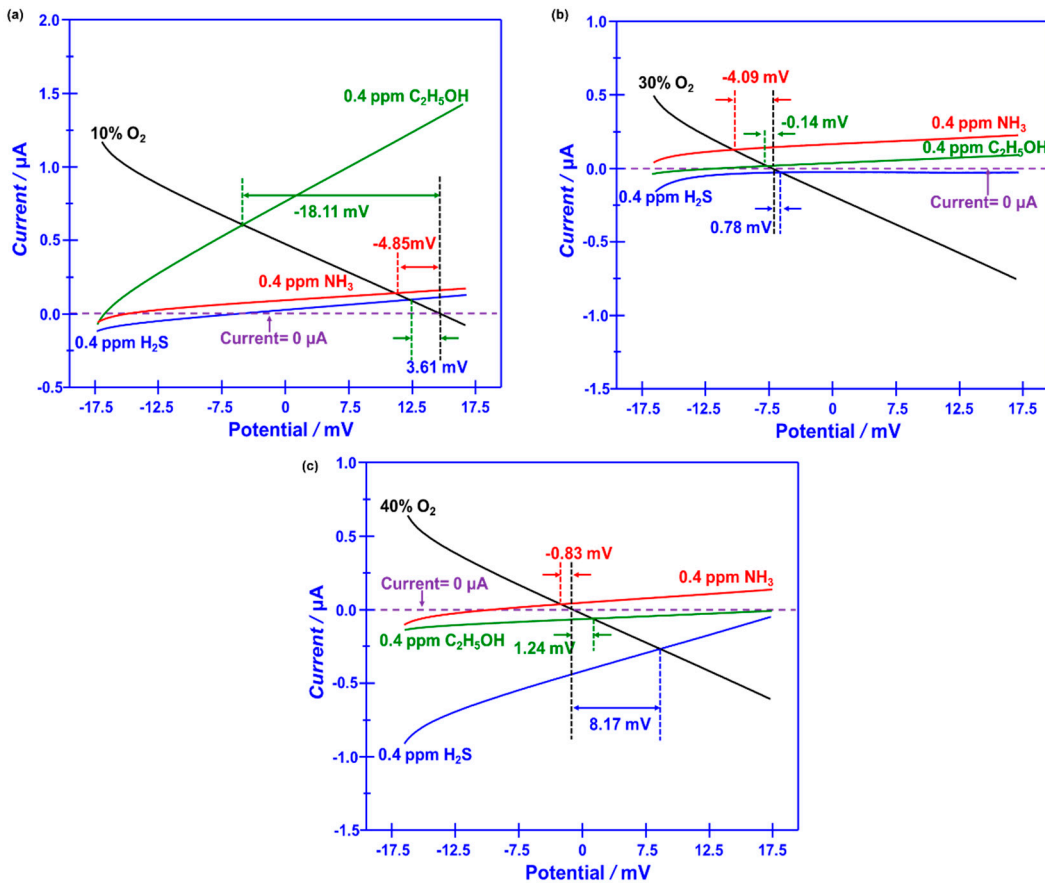
**Figure 4.** Impact of the calcination temperature on the sensing performance of the sensor attached with  $\text{Cr}_2\text{O}_3$ -SE.

Figure 5(a) demonstrate the dependence of the response signal on the concentration of the studied gases for the YSZ-based sensor using  $\text{Cr}_2\text{O}_3$ -SE (calcined at 1000 °C), in the range of 0.04–2 ppm that examined at different oxygen concentration. The linear relationship between the response signal and the logarithm of the gas concentration is observed for the sensor, regardless of the oxygen concentration contained in the gas mixture. Particularly, acceptable selectivity is also confirmed for the sensor by modulating the oxygen concentration. To further confirm the gas sensing specificity, a comparison of the response signal to the 0.04 ppm single gas (e.g.  $\text{H}_2\text{S}$ ,  $\text{NH}_3$ ,  $\text{C}_2\text{H}_5\text{OH}$ ) and the gas mixture (target gas + 2 ppm interference gases) is investigated and shown in Figure 5(b). Acceptable

specificity is confirmed for the sensor when sensing various targeted gases under different oxygen content. These impressive results directly indicate that the selectivity of the proposed YSZ-based sensor that uses  $\text{Cr}_2\text{O}_3$ -SE is successfully tailored by simply modulating oxygen content in the tested environment. As for the tailored selectivity of the sensor, it can be interpreted through the standard modified polarization curves that are given in Figure 6. The difference in the modified polarization curves for each studied target gas at the oxygen concentration of 10-40% suggests that the interfacial catalytic activity of the sensor changed with the variation of the oxygen concentration. Particularly, due to the mixed potential behavior of the sensor, distinct different sensing behavior is obtained when modulating the oxygen concentration in the gas mixture.



**Figure 5.** (a) dependence of the response signal on the concentration of the studied gases for the sensor using  $\text{Cr}_2\text{O}_3$ -SE, in the range of 0.04–2 ppm is examined at different oxygen concentrations; (b) dependence of the response signal on the concentration of the studied gases for the sensor using  $\text{Cr}_2\text{O}_3$ -SE, in the range of 0.04–2 ppm is examined at different oxygen concentration (b) Comparison of the response signal for the smart gas sensor to the studied gas mixture.



**Figure 6.** (a-c) Standard modified polarization curves, measured in 0.04 ppm H<sub>2</sub>S, NH<sub>3</sub>, C<sub>2</sub>H<sub>5</sub>OH under different oxygen concentration values over the range of 10–40 vol.% (with intervals of around 10 vol.-%), for the smart gas sensor coupled with Cr<sub>2</sub>O<sub>3</sub>-SE and Mn-based RE.

Beyond the satisfactory selectivity, quick response/recovery rate and humidity resistance are also crucial technical indexes, since the research objective of this study is tracking target volatile compounds that are generated during food spoilage. Figure 7(a-c) shows the response/recovery state, the 90% response/recovery time of the sensor to H<sub>2</sub>S, NH<sub>3</sub>, and C<sub>2</sub>H<sub>5</sub>OH is 23.6s/17.1s, 7.3s/11.2s and 5.4s/15.2s, respectively, indicating acceptable response/recovery speed for sensing these gases. Meanwhile, water vapor has a negligible impact on the response behavior of the sensor and acceptable stability is confirmed for the sensor (Figure 7d, e). Based on these promising results, it is reasonable to give the conclusion: the smart sensor that integrated oxygen pump membrane and miniaturized YSZ-based gas sensor (attached with Cr<sub>2</sub>O<sub>3</sub>-SE and Mn-based RE) shows excellent oxygen concentration modulation capability and satisfactory gas sensing characteristics, thus, could be a potential candidate for food freshness evaluation.

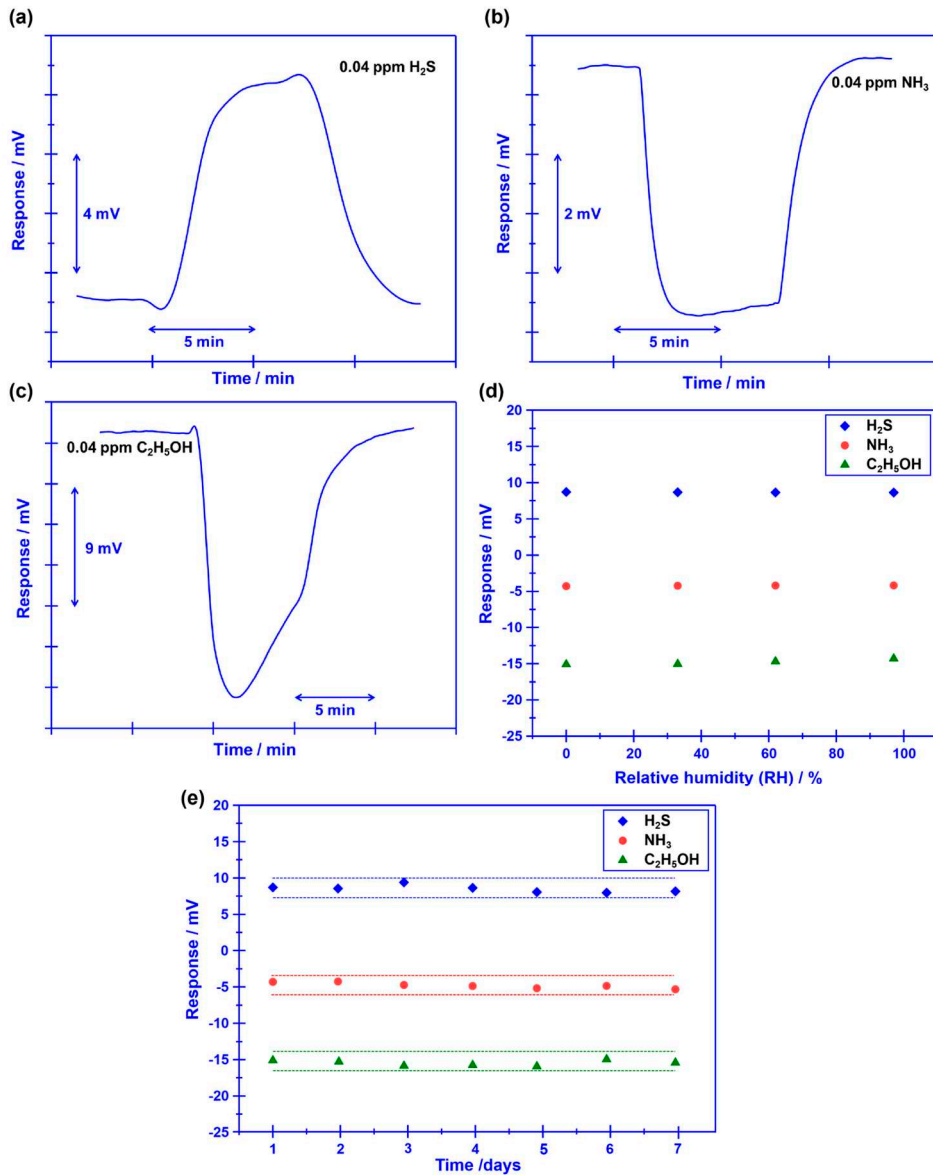


**Figure 7.** (a-c) 90% response/recovery time of the sensor that uses Cr<sub>2</sub>O<sub>3</sub>-SE to H<sub>2</sub>S, NH<sub>3</sub>, and C<sub>2</sub>H<sub>5</sub>OH. (d) Impact of water vapor on the response behavior of the sensor using Cr<sub>2</sub>O<sub>3</sub>-SE. (e) Stability of the sensor to various gases within 1 week.

### 3.3. Capability of real-time monitoring of food freshness

To evaluate the practicability of employing the proposed sensor in freshness monitoring, a refrigerator prototype that includes the smart gas sensor is built and its performance is also examined. It should be particularly noted that to effectively eliminate potential interference derived from other gases (e.g. CO, NO<sub>2</sub>, NO, and SO<sub>2</sub>), commercialized catalyst powder (C21900, Minstrong Tech., China) is placed in front of the sensing chamber to remove potential interference gases. Figure 8a demonstrates the photograph of the designed prototype. The prototype includes a sensing chamber (placing the smart gas sensor), min-pump (sucking in gas derived from food), catalyst tank (placing commercialized catalyst powder), and other refrigerator modules. When the prototype works, gas species in a fresh room would be automatically pumped into the sensing chamber and examined by the sensor. Figure 8b gives the conversion rate of each gas, calculated by comparing the concentration difference before and after the gas passing through the catalyst. The catalyst essentially removed those potential interference gases, due to the high conversion rate to CO, NO<sub>2</sub>, NO, and SO<sub>2</sub>. Therefore, the smart gas sensor placed behind the catalyst tank reveals a high response signal to H<sub>2</sub>S, NH<sub>3</sub>, and C<sub>2</sub>H<sub>5</sub>OH against the aforementioned interference gases (Figure 8c). Consequently, it is

believed that the designed prototype would be capable of alarming food spoilage by simply tracking volatile compounds.

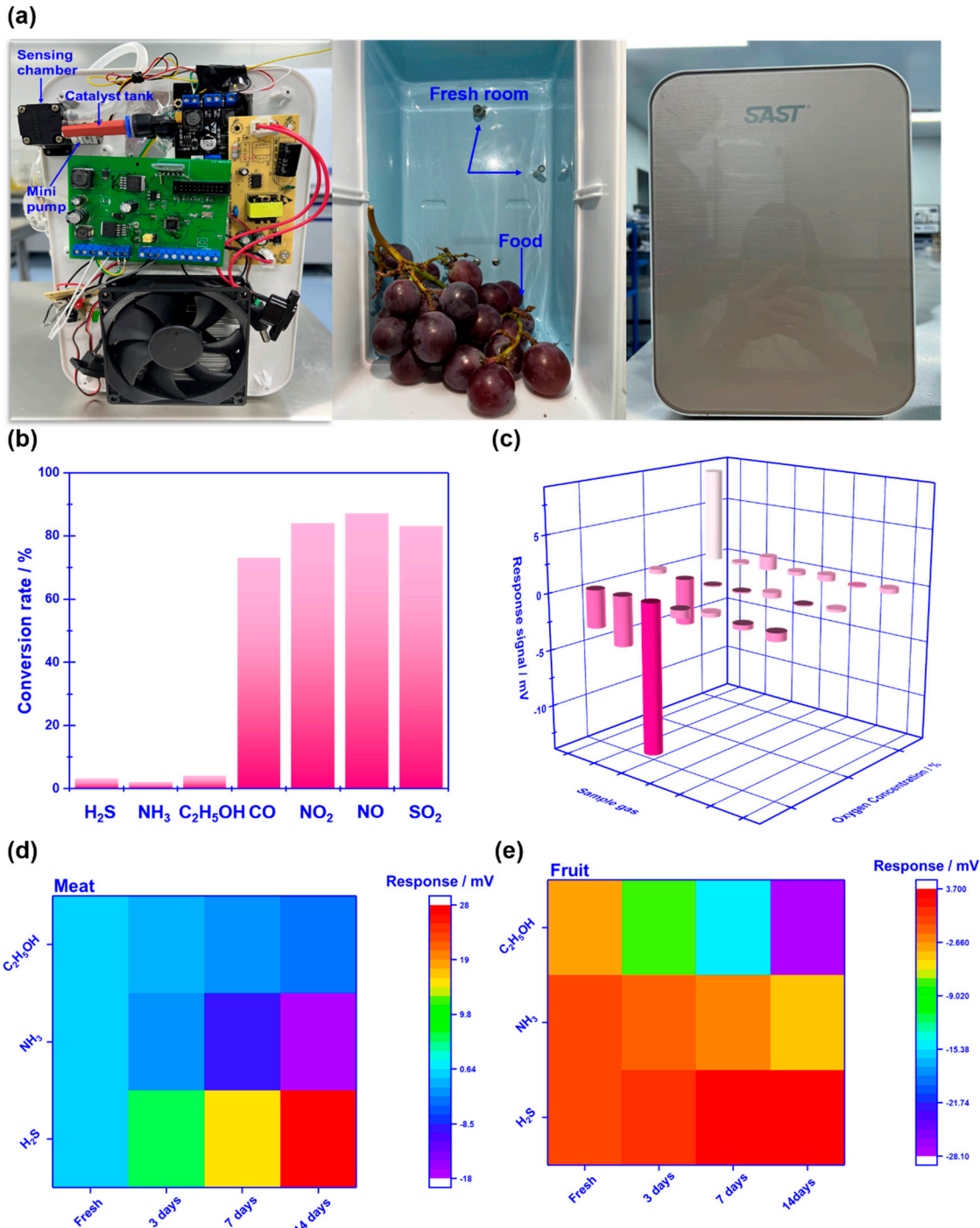


**Figure 8. Photograph and sensing performance of the refrigerator prototype:** (a) internal details of the refrigerator prototype; (b) comparison of the conversion rate for the studied gases before and after passing through the catalyst; (c) response signal of the integrated smart gas sensor against potential interference gases with the help of the commercialized catalyst; (d), (e) variation of the response signal to H<sub>2</sub>S, NH<sub>3</sub>, C<sub>2</sub>H<sub>5</sub>OH in the form of heat map, during the studied 14 days.

Pork, banana, and strawberry are selected as the research examples of meat and fruit to test the performance of the prototype. The above-mentioned foods are kept in a fresh room with the temperature set at 4°C for 0-14 days. The variation of the response signal to the gases sucked from the fresh room is continuously recorded during the tested period. It is found that when keeping these

foods in a fresh room for more than 7 days, obvious color change can be caught in the photograph (Figure 9), suggesting the food spoilage started. Figure 8c, d shows a variation of the response signal to  $\text{H}_2\text{S}$ ,  $\text{NH}_3$ , and  $\text{C}_2\text{H}_5\text{OH}$  in the form of a heat map, during the studied 14 days. In sum, according to the variation of the response signal, it can be deduced that significantly increasing in  $\text{H}_2\text{S}$ ,  $\text{NH}_3$  is found during meat spoilage, while for fruit spoilage gas concentration increment is mainly found in  $\text{C}_2\text{H}_5\text{OH}$ . Figure 10 summarizes the pilot results of freshness monitoring by utilizing the designed refrigerator prototype. In this research, the principal components analysis (PCA) method is employed to discriminate the status of fresh (kept within half a day) or semi-fresh (kept more than 3.5 days). Response signal of  $\text{H}_2\text{S}$  and  $\text{NH}_3$  for the meat kept for 3.5 days is around 11.2 mV and -7.4 mV, respectively, while the value of  $\text{C}_2\text{H}_5\text{OH}$  for fruit at the semi-fresh status is roughly estimated to be -19.4 mV. These results depicted in the form of a PCA map imply the satisfactory capability of the prototype to distinguish food freshness, particularly when the experimental sample is meat. Conclusively, the prototype that integrated with the smart gas sensor successfully implemented online freshness monitoring and would provide an effective strategy for alarming food spoilage.



Figure 9. Photograph of pork and selected fruits that were kept for different times.

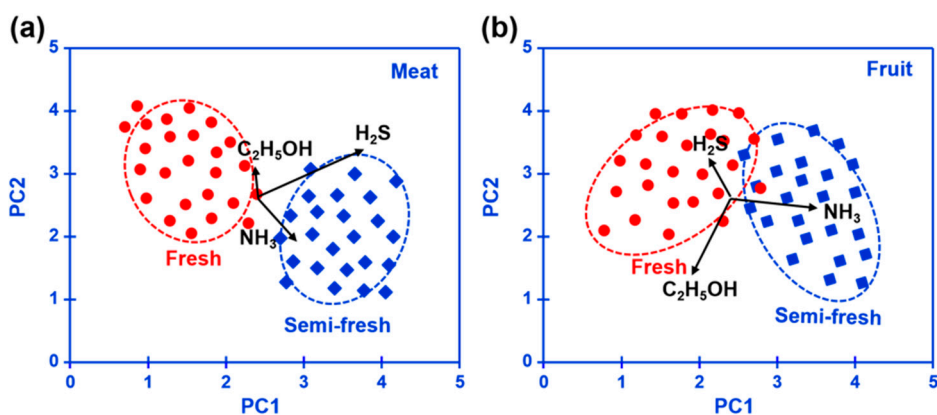


Figure 10. Pilot results of the (a) meat and (b) fruit freshness monitoring for the designed refrigerator prototype, depicted in the form of a PCA map.

#### 4. Conclusions

An integrated smart gas sensor is designed and fabricated for real-time monitoring of food freshness. By applying the pumping voltage on the YSZ membrane, the oxygen concentration in the testing chamber is artificially controlled. Due to the mixed potential behavior, the YSZ-based smart gas sensor that is affixed to  $\text{Cr}_2\text{O}_3$ -SE and Mn-based RE exhibits distinct different sensing

characteristics at different oxygen concentrations. The sensor exhibits satisfactory selectivity for  $\text{H}_2\text{S}$ ,  $\text{NH}_3$ , and  $\text{C}_2\text{H}_5\text{OH}$  at oxygen concentrations of 10%, 30%, and 40%, respectively, in the gas mixture. In addition, an acceptable response/recovery rate is further confirmed for the sensor.

To verify the capability of monitoring the food freshness for the proposed integrated smart gas sensor, a refrigerator prototype that includes the smart gas sensor is built. With the help of commercialized catalysts, high selectivity to these target gases (*i.e.*  $\text{H}_2\text{S}$ ,  $\text{NH}_3$ , and  $\text{C}_2\text{H}_5\text{OH}$ ) that are emitted during food spoilage. Moreover, satisfactory performance in discriminating food freshness status of fresh or semi-fresh is further confirmed for the proposed refrigerator prototype. Conclusively, these promising results suggest that the proposed integrated smart gas sensor could be a potential candidate for alarming food spoilage. Particularly, the strategy of modulating response selectivity through tailoring the oxygen concentration would be a useful way to design future high-performance gas sensors.

**Author Contributions:** Conceptualization, Y.W. and H.J.; methodology, Y.X.; software, Z.L.; validation, N.D.H, N.V.H and A.A.G; formal analysis, J.L.; investigation, J.Z.; resources, V.C.; data curation, A.J.; writing—original draft preparation, Y.X., Z.L., J.L.; writing—review and editing, Y.W., H.J.; visualization, N.D.H, N.V.H and A.A.G.; supervision, D.C.; project administration, Y.W.; funding acquisition, H.J.; All authors have read and agreed to the published version of the manuscript.

**Funding:** This work was financially supported by National Natural Science Foundation of China (2022YFE0118800, 62227815,52000133), Shanghai Natural Science Foundation (WF220403061), the Belt and Road" young scientist exchange program of the Science and Technology Commission of Shanghai (20490743000), Sichuan Natural Science Foundation (2022NSFSC0390, KX002), Oceanic Interdisciplinary Program of Shanghai Jiao Tong University (SL2020MS014) and Program of National Key Laboratory (SKLPBS2249).

**Acknowledgment:** The authors gratefully acknowledge the support for this research from Yuyao Wu, Chenhan Yi, Cuili Xue, Yuna Zhang, Shan Gao, and Kistenev Yury V.

**Conflicts of Interest:** The authors declare no conflict of interest.

## Appendix A

TOC



## References

1. Preethichandra, D.; Gholami, M.D.; Izake, E.L.; O'Mullane, A.P.; Sonar, P. Conducting Polymer Based Ammonia and Hydrogen Sulfide Chemical Sensors and Their Suitability for Detecting Food Spoilage. *Advanced Materials Technologies* **2023**, *8*, 2200841.
2. Sequino, G.; Valentino, V.; Villani, F.; De Filippis, F. Omics-based monitoring of microbial dynamics across the food chain for the improvement of food safety and quality. *Food Research International* **2022**, *157*, 111242, doi:<https://doi.org/10.1016/j.foodres.2022.111242>.
3. Odeyemi, O.A.; Alegbeleye, O.O.; Strateva, M.; Stratev, D. Understanding spoilage microbial community and spoilage mechanisms in foods of animal origin. *Compr Rev Food Sci Food Saf* **2020**, *19*, 311-331, doi:10.1111/1541-4337.12526.
4. Lin, Z.-Y.; Xue, S.-F.; Chen, Z.-H.; Han, X.-Y.; Shi, G.; Zhang, M. Bioinspired copolymers based nose/tongue-mimic chemosensor for label-free fluorescent pattern discrimination of metal ions in biofluids. *Analytical chemistry* **2018**, *90*, 8248-8253.
5. in't Veld, J.H.H. Microbial and biochemical spoilage of foods: an overview. *International journal of Food microbiology* **1996**, *33*, 1-18.
6. Edita, R.; Darius, G.; Vinauskienė, R.; Eisinaité, V.; Balčiūnas, G.; Dobilienė, J.; Tamkutė, L. Rapid evaluation of fresh chicken meat quality by electronic nose. *Czech Journal of Food Sciences* **2018**, *36*, 420-426.
7. Peris, M.; Escuder-Gilabert, L. A 21st century technique for food control: Electronic noses. *Analytica chimica acta* **2009**, *638*, 1-15.
8. Wang, S.; Chen, H.; Sun, B. Recent progress in food flavor analysis using gas chromatography-ion mobility spectrometry (GC-IMS). *Food Chemistry* **2020**, *315*, 126158.
9. Shaik, M.I.; Azhari, M.F.; Sarbon, N.M. Gelatin-based film as a color indicator in food-spoilage observation: a review. *Foods* **2022**, *11*, 3797.
10. Sonwani, E.; Bansal, U.; Alroobaee, R.; Baqasah, A.M.; Hedabou, M. An Artificial Intelligence Approach Toward Food Spoilage Detection and Analysis. *Frontiers in Public Health* **2022**, *9*, 816226.
11. Peng, X.; Liu, J.; Tan, Y.; Mo, R.; Zhang, Y. A CuO thin film type sensor via inkjet printing technology with high reproducibility for ppb-level formaldehyde detection. *Sensors and Actuators B: Chemical* **2022**, *362*, 131775.
12. Wang, M.; Gao, F.; Wu, Q.; Zhang, J.; Xue, Y.; Wan, H.; Wang, P. Real-time assessment of food freshness in refrigerators based on a miniaturized electronic nose. *Analytical Methods* **2018**, *10*, 4741-4749.
13. Yuan, Z.; Bariya, M.; Fahad, H.M.; Wu, J.; Han, R.; Gupta, N.; Javey, A. Trace-level, multi-gas detection for food quality assessment based on decorated silicon transistor arrays. *Advanced materials* **2020**, *32*, 1908385.
14. Hu, W.; Wu, W.; Jian, Y.; Haick, H.; Zhang, G.; Qian, Y.; Yuan, M.; Yao, M. Volatolomics in healthcare and its advanced detection technology. *Nano Research* **2022**, *15*, 8185-8213.
15. Lehotay, S.J.; Hajšlová, J. Application of gas chromatography in food analysis. *TrAC Trends in Analytical Chemistry* **2002**, *21*, 686-697, doi:[https://doi.org/10.1016/S0165-9936\(02\)00805-1](https://doi.org/10.1016/S0165-9936(02)00805-1).
16. Tani, A.; Hayward, S.; Hewitt, C.N. Measurement of monoterpenes and related compounds by proton transfer reaction-mass spectrometry (PTR-MS). *International Journal of Mass Spectrometry* **2003**, *223-224*, 561-578, doi:[https://doi.org/10.1016/S1387-3806\(02\)00880-1](https://doi.org/10.1016/S1387-3806(02)00880-1).
17. Zambotti, G.; Soprani, M.; Gobbi, E.; Capuano, R.; Pasqualetti, V.; Natale, C.D.; Ponzoni, A. Early detection of fish degradation by electronic nose. In Proceedings of 2019 IEEE International Symposium on Olfaction and Electronic Nose (ISOEN), 26-29 May 2019; pp. 1-3.
18. Wasilewski, T.; Gębicki, J. Emerging strategies for enhancing detection of explosives by artificial olfaction. *Microchemical Journal* **2021**, *164*, 106025, doi:<https://doi.org/10.1016/j.microc.2021.106025>.
19. Palacín, J.; Rubies, E.; Clotet, E.; Martínez, D. Classification of two volatiles using an eNose composed by an array of 16 single-type miniature micro-machined metal-oxide gas sensors. *Sensors* **2022**, *22*, 1120.
20. Rusinek, R.; Dobrzański Jr, B.; Oniszczuk, A.; Gawrysiak-Witulska, M.; Siger, A.; Karami, H.; Ptaszyńska, A.A.; Żytek, A.; Kapela, K.; Gancarz, M. How to Identify Roast Defects in Coffee Beans Based on the Volatile Compound Profile. *Molecules* **2022**, *27*, 8530.
21. John, A.T.; Murugappan, K.; Nisbet, D.R.; Tricoli, A. An Outlook of Recent Advances in Chemiresistive Sensor-Based Electronic Nose Systems for Food Quality and Environmental Monitoring. In *Sensors*, 2021; Vol. 21.

22. Yuan, Z.; Bariya, M.; Fahad, H.M.; Wu, J.; Han, R.; Gupta, N.; Javey, A. Trace-Level, Multi-Gas Detection for Food Quality Assessment Based on Decorated Silicon Transistor Arrays. *Adv Mater* **2020**, *32*, e1908385, doi:10.1002/adma.201908385.
23. Cui, S.; Yang, L.; Wang, J.; Wang, X. Fabrication of a sensitive gas sensor based on PPy/TiO<sub>2</sub> nanocomposites films by layer-by-layer self-assembly and its application in food storage. *Sensors and Actuators B: Chemical* **2016**, *233*, 337-346.
24. Guo, X.; Ding, Y.; Liang, C.; Du, B.; Zhao, C.; Tan, Y.; Shi, Y.; Zhang, P.; Yang, X.; He, Y. Humidity-activated H<sub>2</sub>S sensor based on SnSe<sub>2</sub>/WO<sub>3</sub> composite for evaluating the spoilage of eggs at room temperature. *Sensors and Actuators B: Chemical* **2022**, *357*, 131424.
25. Sun, Y.; Hu, J.; Zhang, Y. Visible light assisted trace gaseous NO<sub>2</sub> sensor with anti-humidity ability via LSPR enhancement effect. *Sensors and Actuators B: Chemical* **2022**, *367*, 132032.
26. Bekhit, A.E.-D.A.; Holman, B.W.; Giteru, S.G.; Hopkins, D.L. Total volatile basic nitrogen (TVB-N) and its role in meat spoilage: A review. *Trends in Food Science & Technology* **2021**, *109*, 280-302.
27. Shahidi, F.; Hossain, A. Role of lipids in food flavor generation. *Molecules* **2022**, *27*, 5014.
28. Brameld, J.M.; Parr, T.; Bender, D.A. 7 Carbohydrate metabolism. *Human Nutrition* **2023**, *136*.
29. Shaalan, N.M.; Ahmed, F.; Saber, O.; Kumar, S. Gases in food production and monitoring: Recent advances in target chemiresistive gas sensors. *Chemosensors* **2022**, *10*, 338.
30. Sato, T.; Plashnitsa, V.V.; Utiyama, M.; Miura, N. YSZ-based sensor using NiO sensing electrode for detection of volatile organic compounds in ppb level. *Journal of The Electrochemical Society* **2011**, *158*, J175.
31. Tanaka, Y.; Sato, T.; Ikeda, H.; Miura, N. Cobalt-based solid reference-electrode usable in zirconia-based sensors for detection of oxygen or volatile organic compounds. *Sensors and Actuators B: Chemical* **2014**, *203*, 899-903.
32. Cheng, C.; Zou, J.; Zhou, Y.; Wang, Z.; Jin, H.; Xie, G.; Jian, J. Fabrication and electrochemical property of La<sub>0.8</sub>Sr<sub>0.2</sub>MnO<sub>3</sub> and (ZrO<sub>2</sub>) 0.92 (Y<sub>2</sub>O<sub>3</sub>) 0.08 interface for trace alcohols sensor. *Sensors and Actuators B: Chemical* **2021**, *331*, 129421.
33. Hu, J.; Liu, X.; Zhang, J.; Gu, X.; Zhang, Y. Plasmon-activated NO<sub>2</sub> sensor based on Au@ MoS<sub>2</sub> core-shell nanoparticles with heightened sensitivity and full recoverability. *Sensors and Actuators B: Chemical* **2023**, *382*, 133505.
34. Jian, Y.; Zhang, N.; Liu, T.; Zhu, Y.; Wang, D.; Dong, H.; Guo, L.; Qu, D.; Jiang, X.; Du, T. Artificially intelligent olfaction for fast and noninvasive diagnosis of bladder cancer from urine. *ACS sensors* **2022**, *7*, 1720-1731.
35. Zhang, M.; Sun, J.J.; Khatib, M.; Lin, Z.-Y.; Chen, Z.-H.; Saliba, W.; Gharra, A.I.; Horev, Y.D.; Kloper, V.; Milyutin, Y. Time-space-resolved origami hierarchical electronics for ultrasensitive detection of physical and chemical stimuli. *Nature Communications* **2019**, *10*, 1120.
36. Perera, A.; Pardo, A.; Barretino, D.; Hierlermann, A.; Marco, S. Evaluation of fish spoilage by means of a single metal oxide sensor under temperature modulation. *Sensors and Actuators B: Chemical* **2010**, *146*, 477-482.
37. Ghasemi-Varnamkhasti, M.; Mohtasebi, S.S.; Siadat, M.; Balasubramanian, S. Meat quality assessment by electronic nose (machine olfaction technology). *Sensors* **2009**, *9*, 6058-6083.
38. Matindoust, S.; Farzi, G.; Nejad, M.B.; Shahrokhabadi, M.H. Polymer-based gas sensors to detect meat spoilage: A review. *Reactive and Functional Polymers* **2021**, *165*, 104962.
39. Shaalan, N.M.; Ahmed, F.; Kumar, S.; Melaibari, A.; Hasan, P.M.; Aljaafari, A. Monitoring food spoilage based on a defect-induced multiwall carbon nanotube sensor at room temperature: Preventing food waste. *ACS omega* **2020**, *5*, 30531-30537.
40. Itagaki, Y.; Mori, M.; Sadaoka, Y. EMF response of the YSZ based potentiometric sensors in VOC contaminated air. *Current Opinion in Electrochemistry* **2018**, *11*, 72-77.
41. Sato, T.; Breedon, M.; Miura, N. Selectivity Enhancement of YSZ-based VOC Sensor Utilizing SnO<sub>2</sub>/NiO-SE Via the Application of a Physical Gas-Diffusion Barrier. *ECS Transactions* **2013**, *50*, 129.
42. Kasalizadeh, M.; Khodadadi, A.A.; Mortazavi, Y. Coupled metal oxide-doped Pt/SnO<sub>2</sub> semiconductor and yttria-stabilized zirconia electrochemical sensors for detection of VOCs. *Journal of The Electrochemical Society* **2013**, *160*, B218.
43. Ramaiyan, K.P.; Mukundan, R. Editors' choice—review—recent advances in mixed potential sensors. *Journal of The Electrochemical Society* **2020**, *167*, 037547.

44. Miura, N.; Sato, T.; Anggraini, S.A.; Ikeda, H.; Zhuiykov, S. A review of mixed-potential type zirconia-based gas sensors. *Ionics* **2014**, *20*, 901–925.
45. Jiang, X.; Zou, J.; Ni, Y.; Wang, Y.; Qian, X.; Li, X.; Wei, S.; Su, Y.; Xie, G.; Zhou, M. Synergistic Au passivation and prolonged aging optimization enhance the long-term catalytic stability of porous YSZ/Pt electrodes. *Journal of Alloys and Compounds* **2023**, *940*, 168812.
46. Hu, W.; Wan, L.; Jian, Y.; Ren, C.; Jin, K.; Su, X.; Bai, X.; Haick, H.; Yao, M.; Wu, W. Electronic noses: from advanced materials to sensors aided with data processing. *Advanced Materials Technologies* **2019**, *4*, 1800488.
47. Lin, Q.; Cheng, C.; Zou, J.; Kane, N.; Jin, H.; Zhang, X.; Gao, W.; Jin, Q.; Jian, J. Study of response and recovery rate of YSZ-based electrochemical sensor by laser ablation method. *Ionics* **2020**, *26*, 4163–4169.

**Disclaimer/Publisher's Note:** The statements, opinions and data contained in all publications are solely those of the individual author(s) and contributor(s) and not of MDPI and/or the editor(s). MDPI and/or the editor(s) disclaim responsibility for any injury to people or property resulting from any ideas, methods, instructions or products referred to in the content.